Research Article

An Optimized Design of a Single-Effect Solar Absorption Chiller for Designing an Optimized Energy-Consuming Residential Building

Negin Maftouni*, Kiana Motaghedi

Department of Mechanical Engineering, Faculty of Engineering & Technology, Alzahra University, Deh-Vanak, Tehran, Iran.

ABSTRACT

Traditional fossil fuels, which are also depleting cause environmental problems. A significant portion of global energy consumption is due to building air conditioning systems. Nowadays, considerable attention is drawn to renewable and sustainable energy sources to support the energy requirements of buildings. In this study, a solar absorption chiller was designed for a three-floor residential building in hot and arid climate. At first, thermal loads in the building were calculated using Carrier software. The material and color of the exterior walls, as well as window types, were changed to reduce the heat transfer coefficient and get an optimum design. Results indicate that by using the optimum design, maximum heating load reduction and maximum cooling load reduction can be achieved with approximate rates of 37 % and 12 %, respectively. Considering safety factor and based on the maximum cooling load, a single-effect LiBr-water solar absorption chiller was designed for the optimum building. Two different scenarios were suggested using two types of flat plate and evacuated tube collector. Results show that in the case of evacuated tube collector the net collector area of 254.18 m^2 is sufficient to supply the cooling power. Implementing flat plate collectors would result in occupying an area of 398.5 m^2. Regarding the limitation of total area of roof and efficiency issues, the evacuated tube collector is the best option.

1. INTRODUCTION

The requirements regarding the humidity and thermal comfort in all types of buildings lead to a significant rise in energy consumption. Conventional air conditioning systems usually consume high amount of electrical energy taken from fossil fuel resources. However, with respect to the disadvantages as a result of excessive consumption, alternative energy sources and methods for reducing energy consumption, in general, were highly emphasized. The limits of fossil fuel, environmental concerns, economic growth, greater demand, and political and economic crises have motivated researchers to concentrate on reducing energy consumption so as to prevent as much recurrence of such crises in the future as possible. The World Business Council for Sustainable Development reports that buildings consume about 40 % of total energy in the world [1]. There is a two-branch solution to overcoming this situation: firstly, to move towards putting up buildings with lower levels of energy consumption and, secondly to substitute the conventional energy resources with renewable energies, especially solar energy, as suitable alternatives. Here, the related studies in both mentioned categories will be briefly reviewed in two separate sections. Then, the aim of the present study will be explained at the end of the introduction.

1.1. Studies on building energy optimization

Due to population growth, the demand for both energy and welfare in construction sector has been following its ascending trend for the years to come. Consequently, this has inspired

much research aimed at reducing energy consumption in buildings. Failing to achieve energy productivity in the construction sector is mostly due to the factors' insufficient knowledge that affects energy consumption in a building. In general, the following factors influence energy consumption in any building: weather conditions building exterior, building construction and maintenance operations, building energy systems, its quality of the interior spaces, and inhabitants activities and [2].

In a different study, researchers have evaluated the effect of window type on the thermal load in buildings during the summer and winter. This study investigates the case of four residential buildings located in four different European cities. They compared the performances of the buildings fitted with double-glazed and triple-glazed windows. According to the results, not only did the triple-glazed windows not exhibit any particular advantage over the double-glazed windows in the summer, but also they were better choices in all the studied cases during winter months [3].

Sedineani et al. attempted to reduce energy consumption in buildings by changing the relevant building parameters. Using different wall materials and two different ceiling models, they compared the respective performances of the studied buildings. The results show that climatic and meteorological conditions play a significant role in selecting building components and designing optimal buildings [4].

Examining the absorption coefficient of different colors used for painting the external walls of the studied building in Mashhad, Ibrahimi et al. identified the optimal color of these walls (that would result in the least amount of energy consumption during a year). They used Gambit to provide 3D models and carry out simulations of the studied building and Fluent to simulate the solar energy radiated by the sun. As the

results show, gray color for a building facade would reduce electricity and gas consumption the year [5].

Climate change also affects buildings' energy consumption. Sajjadian et al. studied the effects of climate change on buildings' energy consumption. To simulate energy consumption by determining the relevant building characteristics, they chose the type of building exterior with the best performance. They also argued that gradual climate change would not affect the initial building design or the system selected for the building [6]. The studies conducted in the field of solar absorption chillers are reviewed in the following subsection.

1.2. Studies on solar absorption chillers

One of the most interesting and applicable renewable energies that could be used to meet buildings' energy requirements is the solar energy, especially the solar absorption chillers as the energy sources that produce air conditioning using solar irradiations. Iran has solar potential higher than the world's average. There are approximately about 300 sunny days in this country, and the solar radiation power is between 1800 and 2200 kW/m^2. Therefore, it is profitable to invest enough research and money resources in developing different solar systems in Iran.

There are some pieces of research in the field of designing solar absorption chillers and, also, evaluating the performance of a solar absorption chiller [7-9]. In 2012, Rosiek et al. [7] studied the performance of a 70 kW single-effect solar LiBr-water chiller and obtained an optimum coefficient of performance (COP) of 0.61, while Ali et al. [9] investigated a 35 kW solar absorption cooling system with the maximum coefficient of performance of 0.81. Yeung et al. [10] designed a 4.7 kW solar absorption chiller with flat plate solar collectors of a total area of 38.2 m² and a storage tank for water. They reported that the collector efficiency was estimated to be 37.5 %. Cullen et al. conducted a research in 2011 [11], indicating that other metrics with capability of saving near 70 % of the total energy are required in all buildings types. Zhai et al. [12] evaluated one of the systems located in China and reported that it was sufficient to provide 70 % of the total cooling load. Wang et al. [13] studied the development and performance of various solar chillers in China and introduced a range of collector efficiencies from 42 % to 60 % and COPs of 0.75-0.81 for the solar absorption cooling machines. Bermejo et al. [14] examined a hybrid solar and gas of double-effect type LiBr-water absorption solar machine and obtained an optimum COP of 40 %. Pongtorn et al. [15] analyzed the performance of a single-effect LiBr-water absorption chiller. The system implemented evacuated solar tubes. In addition, there was a boiler based on liquefied petroleum gas-fired technology to provide heat when there was not enough irradiation. The system was able to supply approximately 80 % of the cooling load. Palacin et al. [16] focused on the influence of a geothermal heating system on a solar chiller and modified the COP by about 18 %. Therefore, if solar energy could be well used for cooling the buildings, energy consumption and emissions would be reduced. In another research, Ghadamian et al. analyzed the thermal energy performance of a flat plate solar collector in order to carry out a sensitivity analysis of effective variables contributing to an approach for increasing performance. To that end, energy and momentum governing equations on a flat plate thermal collector were developed to achieve output air

temperature and velocity profiles. The model theory was validated with experiments by a set of flat plate collectors that were applied to carry out experimental activities. Quantitative results show that the mean differences between the predicted and measured output air temperatures in natural and forced convection cases are 1.47 $^{\circ}C$ (3.5 %) and 0.9 $^{\circ}C$ (1.5 %), respectively. The average error percentages of estimated amounts of output air velocity profile values in natural and forced convection cases were 9 % and 4 %, respectively [17]. The same researchers performed energy modeling and simulation including particle technologies within single- and double-pass solar air heaters to obtain the best performance of the solar air heaters. The results obtained from EES and MATLAB open-source code software are significant and efficient. According to these results, double-pass duct does not necessarily improve the system efficiency. They also indicated that higher ambient air temperature and lower solar irradiation could increase the overall energy efficiency of solar double-pass systems [18].

In addition to these positive results, there are some operational problems and integration issues that limit the development of solar cooling machines compared with that of conventional ones. For instance, compared with the single-effect solar absorption cooling systems, the double-effect types doubled COP; however, they needed a higher operating temperature, i.e., more losses. There is a range of factors, including the collector output temperature, the local climate, the installation angle, etc. that must be taken into account [19]. Some notable pieces of research were done in the field of implementing different nanofluids known as operating fluid [20-23]. Hajabdollahi et al. designed a solar absorption chiller based on hourly analysis [24]. They used Real-Parameter Genetic Algorithms to optimize the system. Ahmed Khan et al. (2018) modeled a single-effect solar chiller in TRNSYS software [25]. Different factors, such as solar fraction and collector efficiency, were assessed to find the optimized variables like storage volume and collector size. Xu et al. studied the implementation of Compound Parabolic Concentrator (CPC) in different single, double, and variable effect solar absorption chillers to find the best option [26]. They found that the variable effect system had high cooling portion, lower heat input, and good efficiency. While the single-effect system showed medium solar portion, higher heat input, and medium efficiency, the double-effect system indicated lower cooling portion, lower heat input, and lower solar efficiency. In another project, a 5 kW-load solar absorption chiller was installed in a university building in Mexico. The operating fluid was the ammonia/lithium nitrate. The absorption cycle produced cooled water that played a role in providing air conditioning. The reported COP varied from 0.28 to 0.48 [27].

Ibrahim et al. worked on a LiBr-water solar absorption cooling machine that was integrated with the energy storage of the same operating fluid [28]. Further, the effects of solar radiation and the coupling energy storage with an absorption chiller will be discussed. The cooling COP of the integrated system is about 0.69, and the energy storage density of the absorption energy storage is 119.6 kWh/m^3.

Hirmiz et al. (2018) developed a Phase Change Materials based on energy storage system integrated with a solar cooling system [29]. The study provides an analytical approach to find appropriate positions and locations of such energy storages. The proposed magnitudes of the analytical approach were validated by the outcomes of a reliable simulation. They

developed an engineering approach to have a better understanding of the predicted value of water and PCM thermal storage of solar cooling systems.

The present study aims to optimize energy saving of a three-floor residential building in hot and dry climate and to design a suitable solar absorption chiller for the optimized building. None of the former studies has embodied these two stages at the same time. Of note, this study aimed at both energy needs reduction design and the greater use of renewable energy resources. First, the thermal loads of the building are computed under different design conditions. Then, building's energy saving is optimized through change of materials, color, and window types. In the second phase, a solar absorption chiller is designed to meet the cooling requirements of the optimized building using renewable energy resource. This approach not only considers building's energy saving, but also less environmental impacts will occur due to substitution of renewable energy resources, which is a valuable movement toward overcoming energy crisis.

2. MATERIALS AND METHODS

The materials and methods of this research can be divided into two parts, namely energetically optimized design and solar absorption chiller development.

2.1. Building optimized design

2.1.1. Building description

A three-storey residential building located in a hot and arid climate is analyzed. Tow-layered internal walls are as follows: the first layer stucco with a thickness of 25 mm and thermal resistance of 0.035 Km^2/W; the second one made of common brick with a thickness of 101.5 mm and a heat conduction coefficient of 0.139 Km^2/W. The roof is made of four layers including gypsum board, RSI-2.5 board insulation, LW concrete block, and ISO insulation with thickness and thermal resistance of 25 mm and 0.121 Km^2/W, 25 mm and 1.22 Km^2/W, 200 mm and 0.355 Km^2/W, and 20 mm and 0.48 Km^2/W, respectively. The external wall is basically made of gypsum board, LW concrete block, and face brick with thicknesses of 25 mm, 200 mm, and 100 mm, and thermal resistance rates of 0.155 Km^2/W, 0.58 Km^2/W, and 0.076 Km^2/W, respectively (State 1). Two insulation layers are examined to reduce the energy loss of external walls and to optimize the building. A plate insulation layer of RSI-1.2 board is added in each layer between gypsum and concrete. The thickness of this layer in States 1 and 2 is 25 mm (State 2) and 50 mm (State 3), respectively. The thermal resistance of the mentioned insulation is 1.22 Km^2/W and 2.44 Km^2/W, respectively. To study the effect of different window types on energy consumption, three various types of single glazed (1), double glazed (2), and reflexing double glazed (3) windows are tested. The doors are wooden with conductive coefficient of 0.46 W/Km. All the materials and related properties were chosen regarding the 19th Section of National Building Laws [30]. The thermal conductivity of the roof is assumed to be 0.423 W/Km, while it is 0.569 W/Km for the floor. The height from floor to top is assumed to be 2.8 m with a heavy-type structure. Table 1 illustrates the building's characteristics description.

2.1.2. Building modeling and simulation

Carrier software (Version 4.52) was used to calculate the thermal loads of the studied building. Carrier's hourly analysis program (HAP) is a computer package used for estimating building loads that compute the annual load applied to a building by the standards set forth by ASHRAE [31]. The thermal loads of the building were computed and variations of the thermal loads of the building with changing window type, material, and color of the external walls were duly studied to determine the maximum loads required by the building in different seasons. In the studied building, every room is assumed to be a separate space whose details are input to Carrier. There is an energy plan for each region at different hours of day and various days of week. The air penetration phenomenon was also considered. Another consideration was fresh air ventilation into the building spaces. In a typical ventilation system, however, an air-handling system is used to supply fresh air to the building, the components of which must be duly specified.

Table 1. Building's characteristics description.

Characteristic	Description
Type	Three-storey residential
Apartments	11 m
Total height	350 m²
Gross floor area	612 m²
Window area	211 m²
Heat transfer coefficient	
Glazing	1.1 W/Km
External walls	0.328 W/Km
Internal core wall	2.8 W/Km

The thermostat data (including the heating and cooling set points) were also input to the software. The design temperatures were set based on the comfort conditions inside the building spaces. The indoor design temperatures for cooling and heating were 25.5 and 21.1 degrees centigrade, respectively. Safety factors including the sensible cooling coefficient, latent cooling coefficient, and heating coefficient were assumed to be 10 %, 15 %, and 20 % respectively [32]. The cooling safety factors increased the rate of incoming and the cooling coil loads. Finally, for each model, the effect of external color (solar absorption coefficient) on the energy consumption of the building was studied. The most important equations applicable in thermal loads calculations are presented here [33]. To calculate thermal conduction load of walls, roof, and windows, Relation 1 was implemented:

$$Q = U.A.\Delta T \tag{1}$$

where U is the heat transfer coefficient of walls and windows, A is the area and ΔT is the temperature difference. The heat transfer due to seams resulting from Equation 2:

$$Q = V.(0.0749 \times \text{correction factor}).0.241.(T_i - T_o) \tag{2}$$

where V is the penetrated air volume.

Equation 3 calculates the Sun radiation heat transfer from the windows to the building:

$$Q = SHG.A.K \tag{3}$$

in which SHG is the total incident solar radiation that windows receive, A is the area of the windows, and K is a combination of factors that can be found in detail in the references. In addition, K is dependent on storage coefficient,

frame coefficient, height, radius coefficient, and net coefficient [33].

Equation 4 calculates cooling loads for the walls (ceiling, external walls, and doors):

$$Q = U.A.\Delta T_e \tag{4}$$

$$\Delta T_e = 0.78 \frac{R_S}{R_m} \Delta T_{em} \left(1 - 0.78 \times \frac{R_S}{R_m}\right) \Delta T_{es} \tag{5}$$

where R_S and R_m are the maximum radiations from the glass in desired conditions and at latitude 40° in July. ΔT_{em} and ΔT_{es} are the equivalent temperature difference for the wall to shadow and wall to sun in the desired conditions, respectively. Equation 6 is used to calculate cooling conductive load of the window:

$$Q = (U \times A)_{window} \times \Delta T \tag{6}$$

Equations 7 and 8 calculate the cooling loads due to brightness and outside air influx:

$$Q = 3.41 \times W \times F_u \times F_s \times CLF \left[\frac{Btu}{hr}\right] \tag{7}$$

$$Q = 1.08 \times V \times (T_o - T_i) \times BF \tag{8}$$

Therefore, all of the thermal loads can be calculated by the software using the above-mentioned governing equations.

2.2. The design of solar absorption chiller

There are two types of absorption chillers, i.e., single-effect and double-effect, which are different in the number of generators. The single-effect absorption chillers can cool down water temperature from 5 to 10 ^{o}C, which is suitable for residential buildings. LiBr-water and water-ammonia are among the most common fluids in absorption chillers. The temperature in cold water resulting from LiBr-water is above +5 ^{o}C, hence suitable for cooling residential buildings.

The most significant part of designing a solar system is its collector. Solar collectors absorb solar energy as the input and convert it into thermal energy to heat the transfer fluids entering the generator. The high costs of mobile collectors make them inappropriate for residential buildings. In this study, two types of collectors including flat plate and evacuated tube collectors were simulated, and the results were compared. First, in designing a collector, the amount of solar radiation reflected on the collector surface should be determined. Following astronomical, geometric, geographic, and meteorological factors of the region, including sine of the declination angle, air pressure, earth temperature, daily mean air temperature, daily mean maximum dew-point temperature, daily mean relative humidity, real sunshine hours, and daily mean radiation intensity above the atmosphere, also affect the amount of solar radiation. Among these factors, the sine of the declination angle and sunshine hours have the highest and lowest impacts, respectively [34].

The amount of solar radiation depends on the latitude, day of the year, and angle of collector panels. The collector set was designed for climatic conditions of July, i.e., the hottest time of the year, instead of the maximum solar radiation in the summer. Here, the assumed date for solar radiation rate measurement was the 20th of July when residential ventilation reaches its maximum rate based on the Carrier's Hourly Analysis Program (HAP).

The relations usually used for solar calculations are as follows [35].

$$N = integer\left\{\left[275\left(\frac{m}{9}\right) - 30 + i\right] - 2\right\} \tag{9}$$

in which m is the number of the months, and I is the number of the regarding days.

$$AST = LST + ET \pm 4(SL - LL) - DS \tag{10}$$

where LL is the local longitude, SL is the standard longitude, AST is the apparent solar time, LST is the local standard time, DS is the day light saving, and ET is:

$$ET = 9.87 \sin(2B) - 7.33 \cos(B) - 1.5\sin(B) \text{ [min]} \tag{11}$$

$$B = (N - 81)\frac{360}{364} \tag{12}$$

The declination angle is obtained in degrees as follows:

$$\delta = 23.45\sin[\frac{360}{365}(284 + N)] \tag{13}$$

The hour angle in degree is calculated as follows:

$$h = \pm 0.25(\text{minutes from local solar noon}) \tag{14}$$

$$h_{ss} = \cos^{-1}[-\tan(l)\tan(\delta)] \tag{15}$$

Solar altitude angle, α, and solar zenith angle, are as follows:

$$\sin(\alpha) = \cos(\varphi) = \sin(l)\sin(\delta) + \cos(l)\cos(\delta)\cos(h) \tag{16}$$

$$\varphi + \alpha = 90 \tag{17}$$

The angle of incidence, θ, results from:

$$\begin{aligned}\cos(\theta) = &\sin(\delta)\cos(\beta) - \cos(l)\sin(\delta)\sin(\beta)\cos(z_s) + \\ &\cos(l)\cos(\delta)\cos(h)\cos(\beta) + \\ &\sin(l)\cos(\delta)\cos(h)\sin(\beta)\cos(z_s) + \\ &\cos(\delta)\sin(h)\sin(\beta)\sin(z_s)\end{aligned} \tag{18}$$

where β is the surface tilt angle from the horizon, and Z_s is south-facing, tilted surface in the Northern Hemisphere.

The measured solar radiation on the plane perpendicular to the radiation on a specific day is:

$$Gon = Gsc\left(1 + 0.33\cos\left(\frac{360*N}{365}\right)\right)\left[\frac{w}{m^2}\right] \tag{19}$$

Solar radiation on the plane parallel to the surface of the Earth from sunrise to sunset results from:

$$\begin{aligned}HO = &\frac{24*3600}{\pi} * Gon * \left(\cos(l)\cos(\delta)\sin(h) + \right.\\ &\left.\frac{\pi*h_{ss}}{180} * \sin(l) * \cos(\delta)\right)\left[\frac{Mj}{m^2}\right]\end{aligned} \tag{20}$$

$$\frac{H}{HO} = K_T \tag{21}$$
For $h_{ss} > 81.4^°$ and $0.3 \leq K_T \leq 0.8$

$$\frac{H_D}{H} = 1.311 - 3.022 * K_T * 3.427 * K_T^2 - 1.821 * K_T^3 \tag{22}$$

$$H_B = H - H_D \tag{23}$$

$$H_t = R_B H_B + H_D\left(\frac{1+\cos\beta}{2}\right) + (H_B + H_D)\rho_G\left(\frac{1-\cos\beta}{2}\right) \tag{24}$$

A set of evacuated tubes (Jiangu Sunrain, China) and flat plate collectors was used as the proposed collector in two scenarios whose results were compared. In the case of the evacuated tube collector, all tubes were assumed to be insulated to minimize energy dissipation during heat transfer between the collectors and warm water tanks.

Equation 25 is usually used for calculating collector's performance [35]:

$$\eta_{collector} = \eta_o - a_{1a} \times \frac{t_m - t_a}{G} - a_{2a} \times \frac{(t_m - t_a)^2}{G} \qquad (25)$$

where η_o, a_{1a}, and a_{2a} are 0.717, 1.52 $\frac{w}{m^2.K}$, and 0.0085 $\frac{w}{m^2.K}$, respectively. Figure 1 is a schematic of the solar chiller system.
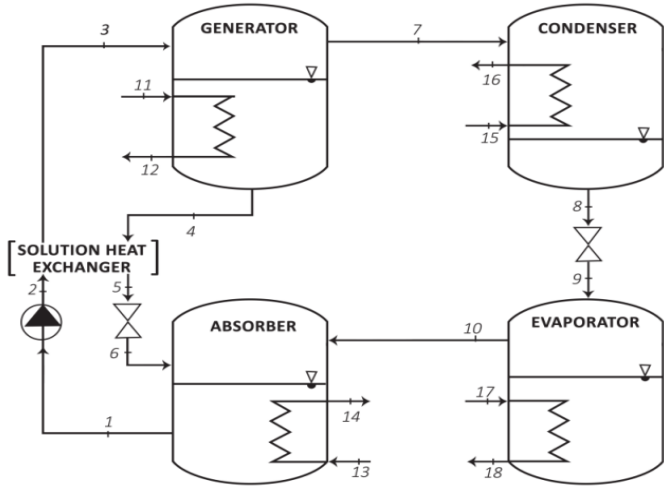

Figure 1. The schematic of the solar chiller system.

The simulation assumptions with respect to the single-effect absorption chiller are as follows: the refrigerant in the condenser's output is saturated liquid (T8); the refrigerant at the operating's exit is saturated vapor (T10); the absorber temperature is the temperature of diluted solution that exits the absorber (T1); the condenser temperature is the temperature of refrigerant that exits the condenser (T8); the generator temperature is the temperature of the solution that exits the generator (T4); there was no thermal exchange between the environment and the system. It is assumed that there is no pressure drop in the elements and pipelines and the electric power consumed by pumps is negligible. The total conservation equation, conservation equation of absorbent, and conservation equation of energy are applicable to all system's elements.

The mass flow of the refrigerant (m_r) is obtained from Equation 26:

$$m_r = \frac{Q_e}{h_{10} - h_9} \qquad (26)$$

The ratio of pump solution mass to that of working fluid is as follows:

$$F_R = \frac{X_{SS}}{X_{SS} - X_{WS}} \qquad (27)$$

where X_{SS} and X_{WS} are the concentrations of diluted and concentrate solution, respectively [36].

The first law of thermodynamics for all chiller's components includes these equations:

$$Q_C = m_r \times (h_7 - h_8) \qquad (28)$$

$$Q_g = m_c h_4 + m_r h_7 - m_d h_2 \qquad (29)$$

$$Q_a = m_c h_6 + m_r h_{10} - m_d h_1 \qquad (30)$$

$$Q_{ex} = m_{ss} \times (h_4 - h_5) = m_{ws} \times (h_3 - h_2) \qquad (31)$$

The efficiency of heat exchanger is as follows:

$$\varepsilon_f = \frac{T_4 - T_5}{T_4 - T_2} \qquad (32)$$

Coefficient of performance of the whole system (COP) can be calculated through Equation 33:

$$COP = \frac{Q_e}{Q_g + W_p} \qquad (33)$$

Ignoring COP of the pump work will results in:

$$COP = \frac{Q_e}{h_7 + (F_R - 1) \times h_4 - (F_R \times h_2)} \qquad (34)$$

All of the above Relations (26-34) are taken from [35]. Table 2 presents inputs used for solar system simulation.

Table 2. Input and constant data for solar chiller.

Parameter	Symbol	Magnitude
Evaporator temperature	$T_e = T_{10}$	7 ^{o}C
Generator temperature	$T_g = T_4$	90 ^{o}C
Absorber temperature	$T_a = T_1$	40 ^{o}C
Condenser temperature	$T_c = T_8$	40 ^{o}C

3. RESULTS AND DISCUSSION

In this section, the results of the former parts of the current research will be presented and discussed. First of all, the results regarding the efforts done to maximize building energy saving are presented in 3.1. Then, the results with respect to designing solar absorption chiller are reported and discussed in 3.2.

3.1. Designing an optimized building

This study aims to optimize cooling and heating energy consumption in a residential building under a hot and arid climate. In this section, efforts were made to reduce energy consumption without affecting the residential comfort level. To this end, the heat transfer coefficient is lowered by means of changing the type of windows and the material and color of external wall layers. The maximum cooling and heating loads are calculated with respect to three external wall models and three window models. The thermal loads for each of these simulated models (according to window type, external wall materials, and color) are calculated. In Figures 2 and 3 the maximum cooling and heating loads of the building are shown in different states, respectively.
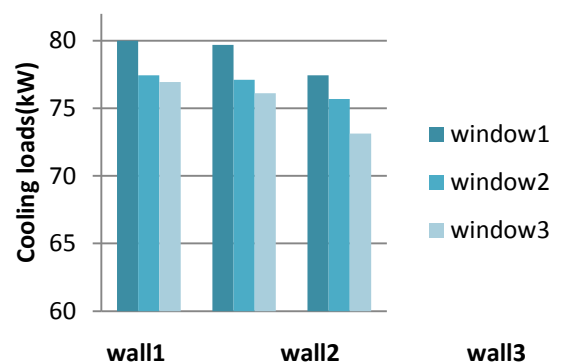

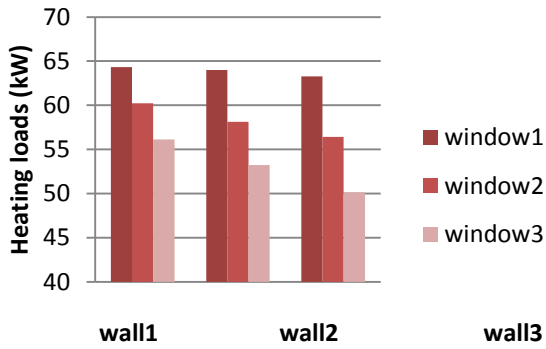**Figure 2.** Maximum cooling loads in different states.

Figure 3. Maximum heating loads in different states.

Tables 3 and 4 report the total yearly cooling and heating loads for all the states including various external walls and window types. Windows 1, 2, and 3 are single-glazed, double-glazed and reflexing double-glazed, respectively. Wall 1 has no insulation, Wall 2 includes the insulation layer with thermal resistance of 1.22 Km^2/W and Wall 3 indicates the wall with the insulation layer of 2.44 Km^2/W thermal resistance.

Table 3. Total yearly cooling loads of the building for all of the states in MWh.

	Window 1	Window 2	Window 3
Wall 1	233,805	243,748	245,682
Wall 2	238,059	245,144	253,561
Wall 3	248,799	254,236	259,505

Table 4. Total yearly heating loads of the building for all of the states in MWh.

	Window 1	Window 2	Window 3
Wall 1	3,398	9,862	25,572
Wall 2	4,193	10,946	27,249
Wall 3	5,754	11,870	28,343

The obtained data indicate that using double-glazed windows with the conduction heat transfer coefficient of 1.1W/Km instead of using single-glazed windows with a heat transfer coefficient of 5.8W/Km leads to an about 5 % reduction in the cooling loads and a 25 % decrease in the heating loads. Changes in the walls also affect the overall load of the building. A comparison of the results shows that changing the materials of external walls reduces the required building load to 4 % and % 9 in the summer and winter, respectively.

Any color change in the outer wall and its effect on the maximum load are simulated. The results show that changing the wall color affects the absorption coefficient and, subsequently, the heating and cooling loads. Three different external wall colors, white, gray, and black, are taken into consideration with the absorption coefficients of 0.45, 0.675, and 0.9, respectively. The simulation results show that any change in the wall color could affect the maximum load. They also indicate that the gray wall with an absorption coefficient of 0.6 is more suitable for this building in all seasons because it reduces the energy requirement to nearly 3 %. Therefore, there is totally 14 % and 39 % energy saving in the cooling and heating modes, respectively. The most notable reason of this notable difference between heating and cooling load savings is the thermal trap. This phenomenon results in preventing energy saving because of double-glazed windows

during the summer. This result shows a similar trend with that obtained by Boyano's [37].

The heating and cooling loads of the first floor of the building were manually calculated to validate the results. Consequently, the cooling loads resulting from manual calculations show about 4 % relative error compared with the simulation results. The relative error for the heating loads was about 5 %.

3.2. Solar Absorption Chiller

The proposed refrigeration system to supply a cooling capacity of 75 kW on the 20th of July is a single-effect LiBr-water absorption chiller with an evacuated tube collector including a 94.6 kW generator in one case and a flat plate collector set in another design.

The amount of the absorbed energy by collectors becomes higher by decreasing the collector slope. The relationship between the collector slope and the amount of energy absorbed by the collector is presented in Figure 4 [35].
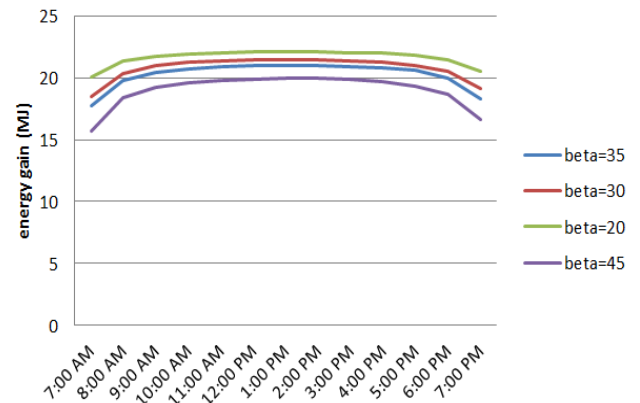

Figure 4. Chart of solar energy absorbed by the collector on different slopes on August 20th.

The optimal slope for the collector is the same as the latitude of the location [35]; therefore, the collectors were allocated with a slope of 35° (β=35) and an azimuth angle of zero (Z_S=0). For this design, the net solar collector area is 254.18 m^2. While the area of the building's ceiling is 420 m^2, the collector's area is logically practical.

Using flat plate collector results in a net area of 398.5 m^2 that is not applicable in this case; therefore, all of the following results would suit the design including evacuated tube collectors.

The chiller's coefficient of performance increases by reducing the absorber and condenser temperatures. The moisture absorption reaction via the LiBr-water is improved by decreasing the absorber temperature, which, in turn, enhances the overall performance of the system. To prevent LiBr-water crystallization in the condenser, cooling is required. Figure 5 reports the trend of COP variation with the absorber temperature.

The chiller's coefficient of performance increases by increasing the generator's temperature. An excessive increase in the generator temperature makes LiBr-water crystallized. The factory coefficient of performance is between 0.7 and 0.78, at which the generator temperature is between 85 °C and 100 °C. In the designed absorption chiller, the generator's temperature is assumed to be 88 °C, at which the chiller's coefficient of performance is 0.778 (Figure 6).
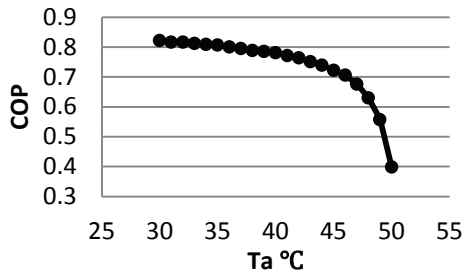
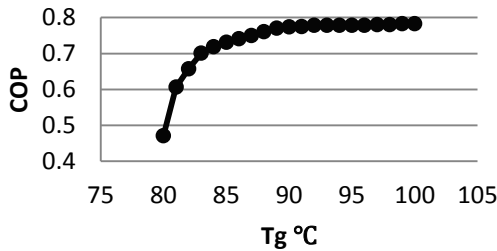**Figure 5.** Variation of COP with the temperature of the absorber.

Figure 6. Variation of COP with the generator temperature when the performance of the heat exchanger is 0.7.

The generated heat reduces as the operating's temperature increases, which, in turn, raises the chiller's coefficient of performance. The chiller's performance is improved by increasing the efficiency of the heat exchanger. The heat exchanger increases the concentrated solution temperature before entering the generator. The exchanger's efficiency increases. Then, the required energy for generator reduces, and the system performance goes up (Figure 7).
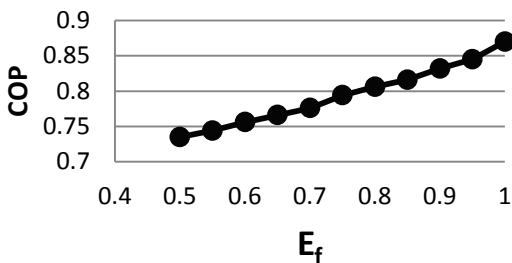

Figure 7. Variation of COP with the effectiveness of heat exchanger.

To validate the results, the findings of the current study were compared to those obtained by Ketfi et al. [38]. Ketfi et al. used MATLAB for simulation. The results obtained were compared with EES (Engineering Equation Solver) simulation results. The variation of EES and MATLAB simulation results is acceptable as seen in Figures 8-10.
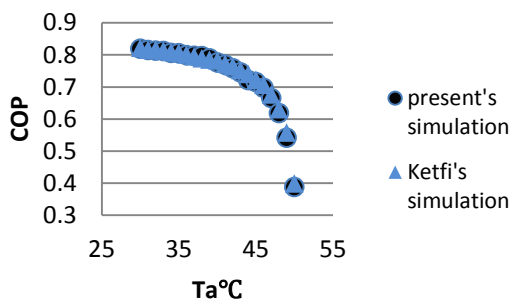

Figure 8. Variations of COP with the absorber temperature for the current study versus those of Ketfi's study.
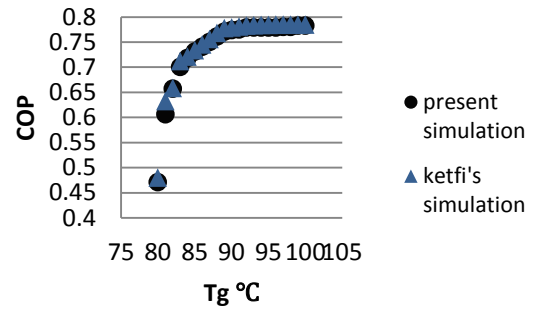

Figure 9. Variations of COP with the generator temperature for the current study versus those of Ketfi's study.
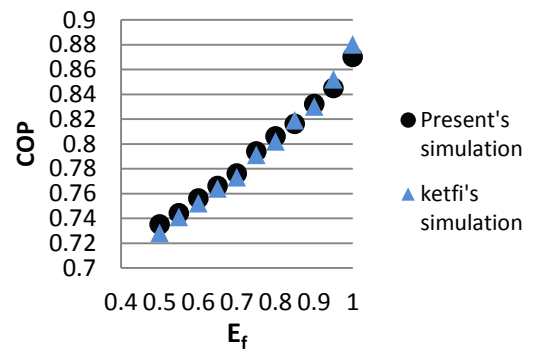

Figure 10. Variations of COP with the effectiveness of heat exchanger for the current study versus those of Ketfi's study.

It is obvious that there is very good agreement between the results of the two pieces of research with respect to COP variations with both absorber's and generator's temperatures. The maximum difference is 4 %.

4. CONCLUSIONS

In this research, a single-effect LiBr-water absorption solar chiller was designed for a three-storey residential building. The effects of changing heat transfer coefficient of the external walls, their color, windows and window awnings application on the maximum load required in the summer and winter were assessed to find the most optimized building design. The changes in the heat transfer coefficient of wall's outer layer had a considerable effect on the maximum heating and cooling loads. In addition, changes in wall color resulted in less change in energy consumption. In the second part of the study, a solar chiller was designed based on maximum thermal loads. An EES code was developed in the scope of the work. Implementing two different types of solar collectors, flat plate and evacuated tube, shows that, depending on using flat plate solar and evacuated tube collectors, net collectors' areas of about 398.5 m^2 and 254.18 m^2 are occupied, respectively, which are sufficient to supply the cooling load of the building in most energy consuming conditions. The simulation results indicate acceptable compatibility with those obtained by the MATLAB simulation of Ketfi et al. research [38]. Finally, it is advisable to use another cooling system alongside the solar chiller to obtain a better package.

5. ACKNOWLEDGEMENT

6. NOMENCLATURE

A	Area (m^2)
AST	Apparent solar time
BF	Shortcut factor
CLF	Cooling load factor
COP	Coefficient of performance
DS	Day light saving
E_f	Heat exchanger effectiveness
F_R	Flow ratio
F_s	Brightness factor
F_u	Usage factor
G_{on}	Extraterrestrial radiation measured on the plane normal to the radiation on the Nth day of the year (W/m^2)
G_{sc}	Solar constant (W/m^2)
h	Hour angle / Enthalpy
h_{ss}	Sunset hour angle
H	Total radiation
H_B	Beam radiation
H_D	Diffuse radiation
HO	Solar radiation on the plane parallel to the surface of the Earth from sunrise to sunset (J/m^2)
I	Number of the regarding day
k_1	Correction factor
k_2	Saving factor
k_3	Window frame factor
k_4	Height factor
k_5	Dew point coefficient
k_6	Cleanliness factor
K_T	Clearness index
LL	Local longitude
LST	Local standard time
m	Mass (kg/s)
M	Number of the month
Q	Transmission heating load / Heat capacity (W)
R_B	Beam radiation tilt factor
R_m	The maximum radiation from the glass for July and the Latitude 40 °
R_s	The maximum radiation from the glass in the desired conditions
SHG	Solar Heat Gain (W/m^2)
SL	Standard longitude
T_i	Indoor dry bulb temperatures (K)
T_o	Outdoor dry bulb temperatures (K)
U	Wall or roof U-value (W/m^2.k)
V	Infiltrate air volume (m^3)
W	Total amount of heat bulbs (Watt)
W_P	Pump work (W)
X	Solution of concentration (%)
Z_s	South-facing, tilted surface in the Northern Hemisphere
α	Solar altitude angle
β	The surface tilt angle from the horizon
φ	Zenith angle
δ	Declination angle
θ	Incident angle
ρ_G	Ground albedo
ΔT_{es}	Equivalent temperature difference for the wall to sun in the desired conditions
ΔT_{em}	Equivalent temperature difference for the wall to shadow in the desired conditions

Indices

a	Absorber
c	Condenser
e	Evaporator
g	Generator
p	Pump
r	Refrigerant
Ss,ws	Strong and weak solutions

REFERENCES

1. http://www.environmentalleader.com/2009/04/27/building-sector-needs-toreduce-energy-use-60-by-2050/.

2. Zhao, H. and Magoules, F., "A review on the prediction of building energy consumption", *Renewable and Sustainable Energy Reviews*, Vol. 16, (2012), 3586–92. (https://doi.org/10.1016/j.rser.2012.02.049).

3. Gasparellaa, A., Pernigottob, G. and Cappellettic, F., "Analysis and modeling of window and glazing systems energy performance for a well-insulated residential building", *Energy and Buildings*, Vol. 43, (2011), 1030–37. (https://doi.org/10.1016/j.enbuild.2010.12.032).

4. Sadineni, B., Madala, S. and Boehm, R.F., "Passive building energy savings: A review of building envelope components", *Renewable and Sustainable Energy Reviews*, Vol. 15, (2011), 3617–31. (https://doi.org/10.1016/j.rser.2011.07.014).

5. Ibrahimi, A., "Study of the effects of external wall's solar absorption coefficient on building energy consumption", *Tabriz Journal of Mechanical Engineering*, Vol. 48, (2018), 34-52.

6. Sajjadian, S.M., Lewisa, J. and Sharples, S., "Energy heating and cooling loads in high performance construction systems- Will climate change alter design decisions?" *Procedia Engineering*, Vol. 118, (2017), 498–506. (https://doi.org/10.1016/j.proeng.2015.08.467).

7. Rosiek, S. and Batlles, F.J., "Integration of the solar thermal energy in the construction: Analysis of the solar e assisted air conditioning system installed in the CIESOL building", *Renewable Energy*, Vol. 34, (2009), 1423-31. (DOI: 10.1016/j.renene.2008.11.021).

8. Ali, A., Noeres, P. and Pollerberg, C., "Performance assessment of an integrated free cooling and solar powered single-effect lithium bromide-water absorption chiller", *Solar Energy*, Vol. 82, (2008), 1021-30. (https://doi.org/10.1016/j.solener.2008.04.011).

9. Darkwa, J., Fraser, S. and Cow, D.H.C., "Theoretical and practical analysis of an integrated solar hot water-powered absorption cooling system", *Energy*, Vol. 39, (2012), 395-402. (https://doi.org/10.1016/j.energy.2011.12.045).

10. Yeung, M.R., Yueu, P.K., Dunn, A. and Cornish, L.S., "Performance of a solar powered air conditioning system in Hong Kong", *Solar Energy*, Vol. 48, (1992), 309-319. (https://doi.org/10.1016/0038-092X(92)90059-J).

11. Cullen, J.M., Allwood, M. and Borgstein, E.H., "Reducing energy demand: What are the practical limits?", *Environmental Science and Technology*, Vol. 43, (2011), 1711-18. (https://doi.org/10.1016/j.rser.2015.03.002).

12. Zhai, X.Q., Wang, R.Z., Wu, J.Y., Dai, Y.J. and Ma, Q. "Solar integrated energy system for a green building", *Energy and Buildings*, Vol. 39, (2007), 985-93. (https://doi.org/10.1016/j.enbuild.2006.11.010).

13. Wang, R.Z. and Zhai, X.Q., "Development of solar thermal technologies in China", *Energy*, Vol. 35, (2010), 4407-16. (https://doi.org/10.1016/j.energy.2009.04.005).

14. Bermejo, P., Pino, F.J. and Rosa, F., "Solar absorption cooling plant in Seville", *Solar Energy*, Vol. 84, (2010), 1503-12. (https://doi.org/10.1016/j.solener.2010.05.012).

15. Pongtornkulpanich, A., Thepa, S., Amornkitbamrun, M. and Butcher, C., "Experience with fully operational solar-driven 10 ton LiBr/H$_2$O single-effect absorption cooling system in Thailand", *Renewable Energy*, Vol. 33, (2008), 943-49. (https://doi.org/10.1016/j.renene.2007.09.022).

16. Palacin, F., Monne, C. and Alonso, S., "Improvement of an existing solar powered absorption cooling system by means of dynamic simulation and experimental diagnosis", *Energy*, Vol. 36, (2011), 4109-18. (https://doi.org/10.1016/j.energy.2011.04.035).

17. Esmailie, F., Ghadamian, H. and Aminy, M., "Modeling and simulation of a solar flat plate collector as an air heater considering energy efficiency", *Mechanics and Industry*, Vol. 15, (2014), 455-464. (https://doi.org/10.1051/meca/2014047).

18. Asghari, F.E., Ghadamian, H. and Aminy, M., "Energy modeling and simulation including particle technologies within single and double pass solar air heaters", *Journal of Particle Science and Technology*, Vol. 2, (2016), 95-102. (DOI: 10.22104/JPST.2016.455).

19. IEA, International Energy Agency, On-going research relevant for solar assisted air conditioning systems, Technical Report Task25: Solar assisted air-conditioning of buildings, (2002), http://www.iea-shc.org/task25/publications/Task25-Subtask C-2-final report.pdf.

20. Xu, X., Xu, C., Liu, J., Fang, X. and Zhang, Zh., "A direct absorption solar collector based on a water-ethylene glycol based nanofluid with anti-freeze property and excellent dispersion", *Renewable Energy*, Vol. 133, (2019), 760-769. (https://doi.org/10.1016/j.renene.2018.10.073).

21. Camposa, C., Vascob, D., Anguloa, C., Burdilesa, P., Cardemilc, J. and Palzaa, H., "About the relevance of particle shape and graphene oxide on the behavior of direct absorption solar collectors using metal based nanofluids under different radiation intensities", *Energy Conversion and Management*, Vol. 181, (2019), 247-257. (https://doi.org/10.1016/j.enconman.2018.12.007).

22. Balakin, B.V., Zhdaneev, O.V., Kosinska, A. and Kutsenko, K.V., "Direct absorption solar collector with magnetic nanofluid: CFD model and parametric analysis", *Renewable Energy*, Vol. 136, (2019), 23-32. (https://doi.org/10.1016/j.renene.2018.12.095).

23. Qin, C., Kang, K., Lee, I. and Lee, B.J., "Optimization of a direct absorption solar collector with blended plasmonic nanofluids", *Solar Energy*, Vol. 150, (2017), 512-520. (https://doi.org/10.1016/j.solener.2017.05.007).

24. Hajabdollahi, Z., Dehnavi, M.S. and Hajabdollahi, H., "Optimization of solar absorption cooling system considering hourly analysis", *Renewable Energy and Environment*, Vol. 4, (2017), 11-19.

25. Ahmed Khan, M., Badar, A.W., Talha, T., Wajahat Khan, M. and Butt, F.S., "Configuration based modeling and performance analysis of single effect solar absorption cooling system in TRNSYS", *Energy Conversion and Management*, Vol. 157, (2018), 351-363. (https://doi.org/10.1016/j.enconman.2017.12.024).

26. Xu, Z.Y. and Wang, R.Z., "Comparison of CPC driven solar absorption cooling systems with single, double and variable effect absorption chillers", *Solar Energy*, Vol. 158, (2017), 511-519. (https://doi.org/10.1016/j.solener.2017.10.014).

27. Soto, P., Dominguez-Inzunza, L.A. and Rivera, W., "Preliminary assessment of a solar absorption air conditioning pilot plant", *Case Studies in Thermal Engineering*, Vol. 12, (2018), 672-676. (https://doi.org/10.1016/j.csite.2018.09.001).

28. Ibrahim, N.I., Al-Sulaiman, F.A. and Ani, F.N., "Performance characteristics of a solar driven lithium bromide-water absorption chiller integrated with absorption energy storage", *Energy Conversion and Management*, Vol. 150, (2017), 188-200. (https://doi.org/10.1016/j.enconman.2017.08.015).

29. Hirmiz, R., Lightstone, M.F. and Cotton, J.S., "Performance enhancement of solar absorption cooling systems using thermal energy storage with phase change materials", *Applied Energy*, Vol. 223, (2018), 11-29. (https://doi.org/10.1016/j.apenergy.2018.04.029).

30. 19th Section of National Building Lows, 3rd Edition, Research Center of Building, (2001).

31. ANSI/ASHRAE Standards 62-1: Ventilation for Acceptable Indoor Air Quality, *ASHRAE Standards and Guidelines*, (2004).

32. Esfahan, M.R., Carrier (HAP 4.5) complete guide, 1st Edition, Yazda Publisher, (2012).

33. Tabatabayee, S.M., Building subsystems calculations, 18th Edition, Rouzbahan Publisher, (2015).

34. Sokhansefat, T.M., "Simulation and parametric study of a 5-ton solar absorption cooling system in Tehran", *Energy Conversion and Management*, Vol. 148, (2017), 339-351. (https://doi.org/10.1016/j.enconman.2017.05.070).

35. Duffie, J.A., Solar engineering of thermal processes, 4th Edition, Wiley, (2013).

36. ASHREA fundamentals, Thermodynamics properties of refrigerant, Chapter 30, Inch-Pound Edition, (2009).

37. Boyano, A., Hernandez, P. and Wolf, O., "Energy demands and potential savings in European office buildings: Case studied based on Energy Plus simulation", *Energy and Buildings*, Vol. 65, (2014), 19–28. (https://doi.org/10.1016/j.enbuild.2013.05.039).

38. Ketfi, O., Merzouk, M., Kasbadji Merzouk, N. and El Metenani, S., "Performance of a single effect solar absorption cooling system (Libr-H_2O)", *Energy Procedia*, Vol. 74, (2015), 130-138. (https://doi.org/10.1016/j.egypro.2015.07.534).